Violation of local realism in a high-dimensional two-photon setup with non-integer spiral phase plates

S.S.R. Oemrawsingh, A. Aiello, E.R. Eliel, G. Nienhuis, and J.P. Woerdman

Huygens Laboratory, Leiden University
P.O. Box 9504, 2300 RA Leiden, The Netherlands

We propose a novel setup to investigate the quantum non-locality of orbital angular momentum states living in a high-dimensional Hilbert space. We incorporate non-integer spiral phase plates in spatial analyzers, enabling us to use only two detectors. The resulting setup is somewhat reminiscent of that used to measure polarization entanglement. However, the two-photon states that are produced, are not confined to a 2×2-dimensional Hilbert space, and the setup allows the probing of correlations in a high-dimensional space. For the special case of half-integer spiral phase plates, we predict a violation of the Clauser-Horne-Shimony-Holt version of the Bell inequality ($S \leq 2$), that is even stronger than achievable for two qubits ($S = 2\sqrt{2}$), namely $S = 3\frac{1}{5}$.

PACS numbers: 03.67.Mn, 42.50.Dv

I. INTRODUCTION

Recently, the orbital angular momentum (OAM) of light has drawn considerable interest in the context of quantum information processing. The spatial degrees of freedom involved in OAM [1] provide a high-dimensional alphabet to quantum information processing (i.e. qu$N$its instead of qubits) [2, 3]. Additionally, since OAM is associated with the topology of the electromagnetic field, the use of this observable in quantum entanglement may lead to states that are inherently robust against decoherence [4].

The most popular OAM analyzer when dealing with conservation, correlation and entanglement of OAM consists of a so-called fork hologram [5], i.e. a binary phase hologram containing a fork in its center [6], together with a spatial-mode detector consisting of a single-mode fiber connected to a single-photon detector; such analyzers have been used in the three-dimensional case, i.e. $N = 3$, by Vaziri *et al.*, [3]. In that experiment, proof of entanglement of the OAM degree of freedom of two photons was given by showing that a generalized Bell inequality was violated; this scheme requires 6 detectors, namely 3 in each arm, and one has to measure 3×3 coincidence count rates [3] to perform a measurement for a single setting of the analyzers.

In the present paper, we consider the use of spiral phase plates (SPPs) [7] instead of phase holograms in an OAM entanglement setup, enabling us to investigate high-dimensional entanglement with only *two* detectors. More specifically, we will consider SPPs that impose on an optical beam a *non-integer* OAM expectation value per photon, in units of $\hbar$ [7]. With such devices, combined with single-mode fibers to form quantum-state analyzers, we propose to build an OAM entanglement setup that is reminiscent of the usual setup to measure polarization entanglement [8], where the rotational settings of the analyzers (polarizers in that case) is varied. We will show that it is possible to identify SPP analyzer settings, in the spirit of horizontal and vertical aligned polarizers,

when using *half*-integer SPPs, allowing observation of high-dimensional entanglement ($N > 2$), in contrast to the polarization case ($N = 2$). These claims are supported by calculations; we predict highly non-classical quantum correlations ($S = 3\frac{1}{5}$), i.e. stronger quantum correlation between two photons than the maximum correlation between two qubits ($S = 2\sqrt{2}$).

II. SPIRAL PHASE PLATES

A SPP, shown in Fig. 1(a), is a transparent dielectric plate with a thickness that varies as a smooth ramp, thus phase shifting an incident field linearly with the azimuthal angle θ [7]. As can be seen, the plate carries a screw discontinuity, expressed by the spiraling thickness, and an edge discontinuity, i.e. a radially oriented step with height h_s. The difference between the maximum and minimum phase shift is written as $2\pi\ell$, where ℓ is not necessarily integer; in fact, ℓ depends on depends on the step height h_s, the difference in refractive indices of the SPP and surrounding medium, and the wavelength of the incident light [7]. Thus, a photon propagating through this plate will acquire an OAM with expectation value equal to $\ell\hbar$ [7, 9]. Placing such a plate in the waist of Laguerre-Gaussian beam, the field in the exit plane just behind the plate will be described by

$$\langle r, \theta | \hat{\mathcal{S}}(\ell) | l, p \rangle = u_{\mathrm{LG}}^{lp}(r, \theta) \exp\left(i\ell\theta\right), \qquad (1)$$

where $|l, p\rangle$ are the Laguerre-Gaussian (LG) field states and $\hat{\mathcal{S}}(\ell)$ is the operator representing the effect of the SPP on the input mode. Note that we have neglected the uniform phase shift that is caused by the SPP's base with height h_0, since it acts as a plane-parallel plate. By adding another plane-parallel plate with the appropriate thickness, the total phase shift of these two can be made equal to an integer multiple of 2π.

The function $u_{\mathrm{LG}}^{lp}(r, \theta)$ in Eq. (1) is the complex amplitude of the Laguerre-Gaussian beam in its waist plane,
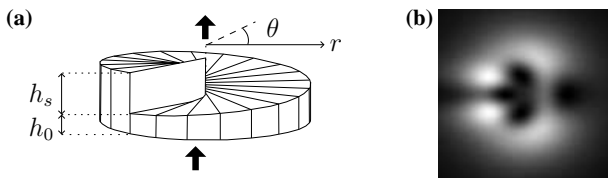
FIG. 1: (a) Schematic drawing of a SPP. The device shifts the phase of an incident beam proportional to the azimuthal angle θ. (b) A calculated far-field diffraction pattern of a fundamental Gaussian beam after propagating through an $\ell = 3\frac{1}{2}$ plate positioned in its waist plane, showing that rotational symmetry is broken. Black and white denote low and high intensity, respectively.

given by [1]

$$\langle r, \theta | l, p \rangle = u_{lp}^{\mathrm{LG}}(r, \theta)$$

$$= C_{lp} \left(-1\right)^p \left(\frac{r\sqrt{2}}{w_0} \right)^{|l|} L_p^{|l|} \left(\frac{2r^2}{w_0^2} \right) \quad (2)$$

$$\times \exp\left(-\frac{r^2}{w_0^2} \right) \exp\left(il\theta \right),$$

where w_0 is the waist radius, $L_p^l(x)$ an associated Laguerre polynomial [10] and C_{lp} a normalization constant. In the paraxial limit, the LG free-space modes, enumerated by the (integer) indices l and p, form a complete basis of spatial modes. The LG index l, which should not be confused with the SPP step index ℓ, is related to the OAM that is carried in that LG mode, namely $l\hbar$ per photon [1, 7, 9], while the index p provides information on the number of nodes along a transverse radius of the mode. When placing a SPP in a beam in a single LG mode, the output will generally be in a *superposition* of LG modes and will be *no* longer *invariant* under free-space propagation. For integer values of the step index ℓ of the SPP, the edge discontinuity is effectively absent and this superposition will only be with respect to the LG-index p [7, 11]. In that case, the intensity distribution of the mode will be doughnut-shaped in the far field. For non-integer ℓ values, the edge discontinuity does not vanish and the superposition of modes will also be with respect to the index l, which is related to the OAM of the mode [7]. Such superpositions consist in principle of an infinite number of LG components. Effectively, this number is finite and increases with ℓ; as an example, if $\ell = \frac{1}{2}$, 11 LG components are sufficient to describe 87% of the field behind the SPP, while for $\ell = \frac{5}{2}$, 224 LG components are required. As SPPs with non-integer ℓ can *create* such high-dimensional superpositions of OAM modes, we anticipate that, when employed suitably, they can also *project* onto such superpositions. We therefore propose to incorporate such non-integer SPPs in analyzers for OAM states living in a high-dimensional Hilbert space.

From a topological point of view, SPPs with non-integer ℓ imprint a mixed screw-edge dislocation on an incident field. The result is rotational asymmetry of the imprinted phase distribution and thus of the emerging field, which becomes visible in the far-field intensity profile (Fig. 1(b)). It is the orientation of the step in the transverse plane, that we wish to exploit as an analyzer setting in a new bipartite entanglement scheme.

Since ℓ shall be chosen to have a non-integer value, it is important to realize that, when an incident field passes through an SPP in combination with its *complement* (i.e. a SPP with the same step height and orientation, but an *inverted* vorticity), the beam basically passes through a plane-parallel plate that shifts the phase of the field, in an azimuthally uniform way, by $2\pi\ell$,

$$\hat{\mathcal{S}}^{\mathrm{compl}}(\ell)\hat{\mathcal{S}}(\ell) = \exp\left(i2\pi\ell\right)\hat{I}, \quad (3)$$

where $\hat{I}$ is the identity operator and where we keep the exponent since $\exp\left(i2\pi\ell\right) \neq 1$ for non-integer ℓ. Since $\hat{\mathcal{S}}(\ell)$ is unitary, it follows that

$$\hat{\mathcal{S}}^{\mathrm{compl}}(\ell) = \exp\left(i2\pi\ell\right)\hat{\mathcal{S}}^{\dagger}(\ell), \quad (4)$$

where $\hat{\mathcal{S}}^{\dagger}(\ell)$ is the Hermitean conjugate of $\hat{\mathcal{S}}(\ell)$. As $\hat{\mathcal{S}}^{\dagger}(\ell)$ and $\hat{\mathcal{S}}^{\mathrm{compl}}(\ell)$ only differ by a multiplicative phase factor we can again use a plane-parallel plate in the experiment to compensate for this phase factor. Similar to the uniform phase shift caused by the SPP's base h_0, we will neglect this phase shift as well, as it can be trivially dealt with. Henceforth, the operator for the compensating SPP, with inverted vorticity, will be represented by the operator $\hat{\mathcal{S}}^{\dagger}(\ell)$.

III. PROPOSAL FOR AN EXPERIMENT

In the experiment on OAM qutrits ($N = 3$), fork holograms were used [3]. Those holograms can only modify the OAM expectation value by an *integer* number [12], depending on the diffraction order of the hologram. It also required the use of *three* analyzers in each arm of a spontaneous parametric down-conversion (SPDC) setup. In contrast, our proposed OAM entanglement experiment uses *non-integer* SPP state detectors and only requires a *single* analyzer-detector combination in each arm. This scheme is shown in Fig. 2; it has been inspired by the setup used in polarization entanglement [8]. The SPPs that are inserted in the two arms should be chosen to obey conservation of OAM (see also section VI). Thus, if the classical pump beam does not contain any OAM, a typical choice for the signal and idler SPPs would be to have step indices ℓ and $-\ell$ respectively, where, in our case, ℓ should have a non-integer value. The role of the lenses in signal and idler path, L_s and L_i respectively, will be discussed in section VI. Finally, single-mode fibers are indicated by F_s and F_i.

By manipulating the transverse axes of our analyzers, namely the SPP steps, we have access to various photon states that live in a high-dimensional OAM Hilbert
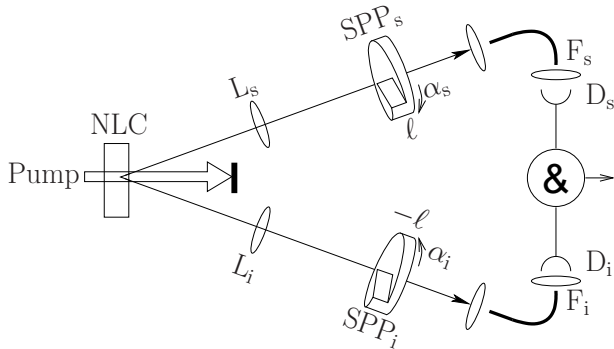
FIG. 2: Proposed experimental setup. A nonlinear crystal (NLC) splits a pump photon in a signal photon and an idler photon by the process of SPDC. In each path, a SPP (SPP$_{s,i}$) is inserted with a single-mode fiber F$_{s,i}$, together forming the analyzer. The coincidence count rate of detectors D$_{s,i}$ is measured as a function of the SPP angular settings α_s and α_i.

space, as mentioned earlier. We may orient these edges arbitrarily in the transverse plane, as shown in Fig. 2, thus allowing their use as angular analyzers. When combined with a single-mode fiber, the SPP with step index ℓ, set at an azimuthal angle α_s, projects the incident photon state out onto the OAM state with expectation value $-\ell$ with edge angle α_s. As we will argue in section VI, the coincidence count rate will depend, like in polarization entanglement, only on the *relative* angle of the transverse axes.

We stress that, in spite of the superficial similarity between a polarizer and a non-integer SPP, they are of course very different devices; for example, while polarization corresponds to *alignment*, the SPP edge corresponds to *orientation*. In other words, with a polarizer, one can analyze the alignment of the electrical field oscillation, either horizontal or vertical, thus yielding a periodicity of π when rotated. With a SPP with non-integer ℓ one can analyze the spatial orientation of a field, thus yielding a periodicity of 2π when rotated (see e.g. Fig. 1(b)). Thus we expect that the coincidence count rate will have a periodicity of 2π when one of our analyzers is rotated.

An equally important difference between the two cases is that, whereas polarization Hilbert space is two dimensional, OAM Hilbert space is infinite dimensional. As we will see, this makes rotation of SPPs fundamentally different from rotation of a polarizer. In order to address these aspects explicitly, we need a basis of the OAM Hilbert space that is suited for our purpose.

IV. NON-INTEGER OAM STATES

Our aim is to construct a complete, orthonormal basis that contains non-integer OAM states as basis elements. To this end, we consider all states in the polar representation and separate the radial and angular parts, so that the arbitrary state $|\vec{r}\rangle = |r, \theta\rangle$ can be written as $|r\rangle|\hat{r}\rangle$,
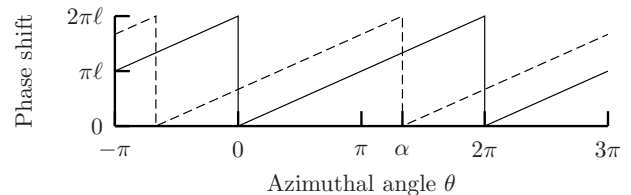

FIG. 3: Plot of the phase shift imprinted by a SPP as a function of the azimuthal angle. The solid line shows this shift for a plate with its edge oriented at $\theta = 0$, while the dashed line shows the phase shift for a plate with its edge at $\theta = \alpha$.

where we have introduced the *direction* (i.e. angular) ket $|\hat{r}\rangle$. This allows us to introduce a complete basis set of angular states, the eigenstates $|l\rangle$ of the OAM operator $\hat{\mathcal{L}}_z$, so that $\hat{\mathcal{L}}_z|l\rangle = l|l\rangle$. A Laguerre-Gaussian state can thus be separated into a radial and angular part, so that $|l, p\rangle = |\rho_{lp}\rangle|l\rangle$, where $|\rho_{lp}\rangle$ is the radial part of the state, which is of less importance in this paper. The OAM eigenstates can be transformed from integer to non-integer OAM states. By applying a unitary operator to the integer OAM basis, its completeness and orthonormality are conserved; the unitary operator that we use is the SPP operator, introduced in Eq. (1):

$$\langle\hat{r}|\hat{\mathcal{S}}(\lambda)|l\rangle \equiv \langle\hat{r}|a_\lambda^{(l)}\rangle = \frac{1}{\sqrt{2\pi}}\exp i(l+\lambda)\theta. \qquad (5)$$

The new basis $\left\{|a_\lambda^{(l)}\rangle\right\}$ has its components enumerated by l, each with OAM equal to $(l+\lambda)\hbar$, where $\lambda \in [0,1)$ is a constant (not to be confused with the wavelength of the light). Different values of λ define different bases of OAM Hilbert space, each basis being complete and orthonormal.

As an example, passing a photon in a fundamental Gaussian mode $|0,0\rangle = |\rho_{00}\rangle|0\rangle$ through a SPP with $\ell = \frac{2}{3}$, creates the state $|\rho_{00}\rangle|a_{2/3}^{(0)}\rangle$; sending this latter photon through a SPP with an aligned step and $\ell = -\frac{2}{3}$, combined with a single-mode fiber, then yields a detection probability of unity.

V. ORIENTATION OF THE EDGE DISLOCATION

Since we intend to rotate the non-integer SPPs, it is important to also have a description of the states that arise when the SPP is rotated while the coordinate system is fixed. To gain insight, we show in Fig. 3 the phase shift imposed by a SPP as a function of the azimuthal angle. The solid line represents the imprinted phase for a SPP with its edge oriented at an angle $\theta = 0$, while the dashed line corresponds to a SPP with edge orientation $\theta = \alpha$. We can now generalize the definition of the operator $\hat{\mathcal{S}}(\ell)$ to the operator $\hat{\mathcal{S}}(\alpha, \ell)$, which includes the

orientation α of the edge dislocation. We find

$$
\begin{aligned}
\langle \hat{r} | \hat{\mathcal{S}}(\alpha, \ell) | l \rangle = & \frac{1}{\sqrt{2\pi}} \exp\left[i(l + \ell)\theta\right] \\
& \times \begin{cases} \exp\left[i(2\pi - \alpha)\ell\right], & 0 \le \theta < \alpha, \\ \exp\left(-i\alpha\ell\right), & \alpha \le \theta < 2\pi, \end{cases}
\end{aligned} \tag{6}
$$

where $\alpha, \theta \in [0, 2\pi)$. This also allows us to generalize the states $|a_\lambda^{(l)}\rangle$ with orientation $\theta = 0$ to states with arbitrary orientation, $|a_\lambda^{(l)}(\alpha)\rangle$. From Eq. (6), it is immediately clear that, when neglecting the uniform phase shift, the complementary SPP operator $\hat{\mathcal{S}}^{\mathrm{compl}}(\alpha, \ell)$ is equal to $\hat{\mathcal{S}}(\alpha, -\ell) = \hat{\mathcal{S}}^\dagger(\alpha, \ell)$.

Since the basis $\left\{ |a_\lambda^{(l)}(0)\rangle \right\}$ is complete, the states after rotation, $|a_\lambda^{(l)}(\alpha)\rangle$ can be written as a superposition of these basis states. Thus the decomposition of $|a_\lambda^{(l)}(\alpha)\rangle$ into the basis $\left\{ |a_\lambda^{(l)}(0)\rangle \right\}$ depends on the angle α. To illustrate this, we make a projection of a non-integer state oriented at $\theta = \alpha$, onto the same state with orientation $\theta = 0$. For this, we choose a SPP with step $\ell = j + \lambda$, where j is the integer part of the step (not to be confused with the integer LG index l), and $\lambda \in [0, 1)$, yielding the overlap amplitude

$$
\begin{aligned}
A_\lambda(\alpha) &= \langle a_\lambda^{(l+j)}(0) | a_\lambda^{(l+j)}(\alpha) \rangle \\
&= \langle l | \hat{\mathcal{S}}^\dagger(0, j + \lambda) \hat{\mathcal{S}}(\alpha, j + \lambda) | l \rangle \\
&= \frac{1}{2\pi} \left[2\pi - \alpha + \alpha \exp\left(i2\pi\lambda\right) \right] \\
&\quad \times \exp\left[-i(l + j + \lambda)\alpha \right],
\end{aligned} \tag{7}
$$

where $|l\rangle$ is the OAM operator eigenstate with eigenvalue l. The overlap probability is then

$$
|A_\lambda(\alpha)|^2 = \left(1 - \frac{\alpha}{\pi}\right)^2 \sin^2\left(\lambda\pi\right) + \cos^2\left(\lambda\pi\right), \tag{8}
$$

which depends neither on the integer part of the step index j nor on the OAM state l. For non-zero values of λ, this overlap function has a quadratic dependence on the orientation α. This function is plotted in Fig. 4 for various values of λ. It illustrates that, when $\lambda = 0$, the projection does not change, as expected. For values of $\lambda \ne 0$, the outcome of the projection is less trivial, with $\lambda = \frac{1}{2}$ providing an especially interesting case: when the state is rotated over $\alpha = \pi$ by rotating the SPP, the state is orthogonal to the non-rotated state. We will call the half-integer states $|a_{\frac{1}{2}}^{(l)}(0)\rangle$ and $|a_{\frac{1}{2}}^{(l)}(\pi)\rangle$ 'up' and 'down', respectively, referring to the orientation of the edge part of the dislocation. In principle, this orientational label can be used for *any* non-integer OAM state, but for half-integer OAM states it carries an analogy to fermionic spin, as our 'up' and 'down' states are orthogonal just like up and down spin $\frac{1}{2}$. In polarization entanglement the comparable orientational labels are known as 'H' for horizontal and 'V' for vertical polarization. To make our proposed OAM entanglement setup maximally equivalent

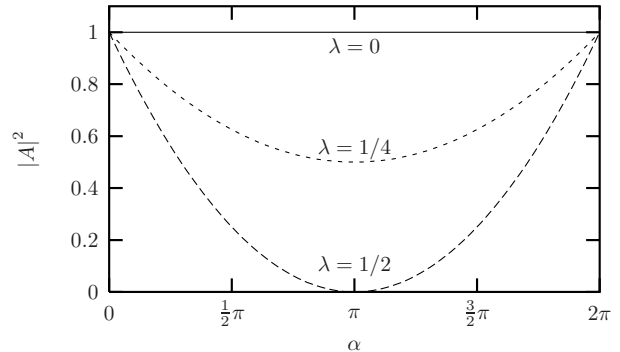FIG. 4: The overlap (see Eq. (8)) between a non-integer OAM state and the identical state rotated over α. When $\lambda = 0$, the states are identical aside from a trivial phase shift, due to the vanishing edge dislocation. For half-integer OAM, i.e. $\lambda = \frac{1}{2}$, the two states are generally different, leading to a parabolic dependence of their overlap; the two states are orthogonal when $\alpha = \pi$.

to the polarizer setup, we focus from now on mainly on the case $\lambda = \frac{1}{2}$. Note that, as Eq. (8) is independent of j, any SPP with $\ell = j + \lambda$ may be used, as long as $\lambda = \frac{1}{2}$.

There is, however, a key difference between the half-integer OAM states on the one hand and the fermionic spin states or polarization states on the other hand. Angularly intermediate states of the fermionic spin or of polarization are a superposition of the two orthogonal basis states 'up' and 'down', or 'H' and 'V', so that the overlap function varies as $\sin^2\alpha$. However, from Eq. (8) we see that in the present case, the dependence of $|A|^2$ on α yields a *parabola*. Thus we conclude that, as the SPP is rotated from 'up' to 'down', the OAM state follows a path through Hilbert space that is *not* confined to the two-dimensional subspace spanned by the 'up' and 'down' states. Note that the OAM expectation value will be conserved along this path, as rotating the SPP has, of course, no effect on its step height, i.e. on ℓ.

VI. ENTANGLEMENT OF HALF-INTEGER ORBITAL ANGULAR MOMENTUM STATES

When dealing with OAM entanglement, issues of conservation of OAM during the spontaneous parametric down-conversion process arise. This conservation is discussed in many papers [2, 13, 14, 15, 16, 17, 18] and it seems that OAM is indeed conserved if two conditions are fulfilled, namely (i) the paraxial limit, and (ii) the thin-crystal limit. In practice this is usually the case and we will therefore work within these limits.

The two-photon state can be described in the spatial polar representation as [19]

$$
|\Psi\rangle = \int d\vec{r}\, \mathcal{P}(\vec{r})\, |\vec{r}\rangle_1 |\vec{r}\rangle_2, \tag{9}
$$

where $\mathcal{P}(\vec{r})$ is the mode function of the pump beam. We restrict ourselves to a pump beam in a pure OAM mode

so that $\mathcal{P}(\vec{r})$ can be written as $\mathcal{P}(r)\exp{(iq\theta)}/\sqrt{2\pi}$, where $\mathcal{P}(r)$ is the radial part of the pump mode function. We can now write the two-photon state in the half-integer SPP basis $\left\{|a_{\frac{1}{2}}^{(n)}(0)\rangle\right\}$, thus yielding

$$
\begin{aligned}
|\Psi\rangle =& \frac{1}{\sqrt{2\pi}}\int \mathrm{d}r\, r\mathcal{P}(r)\,|r\rangle_1\,|r\rangle_2 \\
& \times \sum_{m,n=-\infty}^{\infty}\left[\int\mathrm{d}\theta\,\exp{(iq\theta)}\langle a_{\frac{1}{2}}^{(n)}(0)|\hat{r}\rangle\langle a_{\frac{1}{2}}^{(m)}(0)|\hat{r}\rangle\right] \\
& \times |a_{\frac{1}{2}}^{(n)}(0)\rangle|a_{\frac{1}{2}}^{(m)}(0)\rangle \\
=& \frac{1}{\sqrt{2\pi}}|R\rangle\sum_n |a_{\frac{1}{2}}^{(n)}(0)\rangle\,|a_{\frac{1}{2}}^{(q-n-1)}(0)\rangle,
\end{aligned}
\tag{10}
$$

where we have defined the radial ket,

$$
|R\rangle \equiv \int\mathrm{d}r\, r\mathcal{P}(r)\,|r\rangle_1\,|r\rangle_2.
\tag{11}
$$

We now continue to calculate the coincidence fringe that is expected in the proposed experiment. For the pump beam, we shall assume a fundamental Gaussian beam, so that $q = 0$ in Eq. (10). In the signal path we place an analyzer consisting of a SPP with $\ell = j + \frac{1}{2}$ where j is an integer, with its orientation set to 'up' ($\theta = 0$), represented by $\hat{\mathcal{S}}(0, j + \frac{1}{2})$, and a single-mode fiber. When the detector clicks, the signal state *before* passing through this analyzer is collapsed to $\hat{\mathcal{S}}^{\dagger}(0, j + \frac{1}{2})|0,0\rangle = |\rho_{00}\rangle|a_{\frac{1}{2}}^{(-j-1)}(0)\rangle$, where $|\rho_{00}\rangle$ is the radial part of the fundamental Gaussian state.

Consequently, according to Eq. (10) with $l = 0$, the idler state $|\psi\rangle_2$ is then collapsed to

$$
|\psi\rangle_2 = C|a_{\frac{1}{2}}^{(j)}(0)\rangle,
\tag{12}
$$

where

$$
C = \frac{1}{\sqrt{2\pi}}\left(\langle\rho_{00}|_1\langle\rho_{00}|_2\right)|R\rangle.
\tag{13}
$$

Thus when analysing the idler state with $\hat{\mathcal{S}}(\alpha, j + \frac{1}{2})|0,0\rangle$ we obtain the projection

$$
B(\alpha) = C\langle a_{\frac{1}{2}}^{(j)}(\alpha)|a_{\frac{1}{2}}^{(j)}(0)\rangle.
\tag{14}
$$

Note that Eq. (14) has, aside from a prefactor, exactly the same appearance as Eq. (7) with $\lambda = \frac{1}{2}$. The coincidence fringe is then given by the modulus squared,

$$
|B(\alpha)|^2 = |C|^2\left(1 - \frac{\alpha}{\pi}\right)^2,
\tag{15}
$$

which is proportional to Eq. (8): we find a parabolic coincidence fringe.

The above reasoning to obtain the coincidence fringe $|B(\alpha)|^2$ is valid for any choice of the signal SPP orientation and only depends on the *relative* orientation α of the signal and idler SPPs. Thus a coincidence measurement on entangled OAM pairs using half-integer OAM analyzers, will bring forth a coincidence fringe that is parabolic, regardless of the *individual* settings of the analyzers.

VII.   THE CHSH VERSION OF THE BELL INEQUALITY

There have been several theoretical papers that address the generalization of the Bell inequality [20] to quantify the violation of local realism of two N-dimensional particles (qu$N$its) [3, 21, 22, 23, 24, 25]; an example of a qu$N$it is a spin-s particle with $2s + 1 = N$. It has been pointed out that in this case the use of m_s-sorting devices, such as Stern-Gerlach analyzers, does *not* offer access to higher-dimensional quantum correlations, presumably because the action of a Stern-Gerlach analyzer depends only on the alignment of its quantization axis [23]. Instead of larger spin values ($s > \frac{1}{2}$), the use of spatial degrees of freedom together with Bell multiports has been advocated to gain access to the multidimensional aspects of entanglement [23]. We stress that all this is different from our proposed use of half-integer SPPs ($s + \frac{1}{2}$). These devices do *not* produce finite-N qu$N$its, but imprint the infinite OAM dimensionality of the (oriented) edge on a transmitted light field. Rotation of this edge is equivalent to a partial exploration of the complete Hilbert space along a certain path, namely an iso-OAM path; due to this complexity, it is not clear how a generalized Bell inequality could be applied to our case.

However, instead of using a generalized high-dimensional bipartite Bell inequality, it is allowed to use an inequality for lower-dimensional two-particle entanglement [25]. Thus we choose, as in the polarization case, the inequality introduced by Clauser, Horne, Shimony and Holt (CHSH) for a measurement where the coincidence probability is expected to be a function of only $\alpha_s - \alpha_i$ [26]. When relabelling α_s and α_i as α_1 and α_2 (in no particular order), the CHSH inequality is given by [8, 27]

$$
\begin{aligned}
S =& E(\alpha_1, \alpha_2) - E(\alpha_1', \alpha_2) + E(\alpha_1, \alpha_2') \\
& + E(\alpha_1', \alpha_2') \leq 2.
\end{aligned}
\tag{16}
$$

The function E is specified, for the variables x, y, as [8, 28]

$$
E(x,y) = \frac{P(x,y) + P(x^\perp, y^\perp) - P(x, y^\perp) - P(x^\perp, y)}{P(x,y) + P(x^\perp, y^\perp) + P(x, y^\perp) + P(x^\perp, y)}.
\tag{17}
$$

The notation $x^\perp$ (and similarly for $y^\perp$) is used to indicate an analyzer setting that analyses a state orthogonal to the state with setting x. Thus in our case, $x^\perp \equiv x + \pi$ and $y^\perp \equiv y + \pi$. $P(x,y)$ is the coincidence probability

function, which is equal to

$$P(x,y) = |B(|y - x|)|^2 = C^2 \left(1 - \frac{|y - x|}{\pi}\right)^2. \quad (18)$$

As the periodicity in the present case is half that of the case of polarization entanglement, we use the standard analyzer settings for polarization entanglement [8, 29] multiplied by a factor of two: $\alpha_1 = -\frac{1}{4}\pi$, $\alpha_1' = \frac{1}{4}\pi$, $\alpha_2 = -\frac{1}{2}\pi$, $\alpha_2' = 0$.

Substitution yields a Bell parameter $S = 3\frac{1}{5}$. This is the key result of our paper; it indicates that in the case of entanglement of half-integer OAM states, the maximum violation of the CHSH inequality, given by Eq. (16), is *stronger* than the maximum violation that is allowed in polarization entanglement, namely $S = 2\sqrt{2}$. In other words, quantum non-locality of the photons in the proposed setup is stronger than the maximum achievable for two qubits. To achieve this, only *two* detectors are required and only *one* coincidence count rate is measured per analyzer setting, in contrast to the OAM qu$N$it setup requiring N detectors and N^2 coincidence count rates per analyzer setting [3, 23].

VIII. CONCLUSIONS

In this paper we have put forward a novel approach to demonstrate high-dimensional entanglement of orbital angular momentum states. The proposed setup uses analyzers that consist of non-integer SPPs and single-mode fibers, enabling detection of high-dimensional entanglement with only two detectors.

The key idea is to use the orientation of the edge dislocation in the SPPs. We specialize to the case of half-integer ℓ, so that the orientation of the edge as an analyzer setting can, to a certain extent, be treated similarly as the axis of a polarizer in polarization entanglement. Instead of horizontal and vertical polarization states, we deal with 'up' and 'down' states, referring to the orientation of the edge dislocation. We analytically calculate the coincidence fringe in the entanglement setup and find it to be parabolic in shape, and periodic over 2π. When evaluating the well-known CHSH Bell parameter, we find $S = 3\frac{1}{5}$, i.e. we predict beyond-Bell pairing of two photons. To achieve this, we require only *two* detectors, as opposed to the standard multiport approach [3, 23]. This economic exploitation of the spatial degrees of freedom seems to be a consequence of the singular nature of our half-integer SPPs, which implies, in principle, infinite dimensionality.

Experimental verification of the outlined proposal is under way.

Acknowledgements

We acknowledge M. P. van Exter for fruitful discussions regarding the CHSH version of the Bell inequality.

APPENDIX: PURE EDGE DISLOCATION

In the present paper, we have seen that, for spiral phase plates with half-integer step index ℓ, i.e. imprinting a mixed screw-edge dislocation, the coincidence fringe in a twin-photon experiment is parabolic as a function of the relative orientation of the two radial edges, with visibility equal to 1. This then results in a value of the CHSH-Bell parameter equal to $S = 3\frac{1}{5}$.

An intriguing question is whether there are other devices with optical singularities, besides the half-integer spiral phase plate, that, in a quantum experiment, will give rise to a similarly large value of the S-parameter. More precisely, can one design a twin-photon experiment that results in a value of the S-parameter larger than $2\sqrt{2}$, using devices that are simpler to produce and handle than the spiral phase plate discussed so far?

As we will see below, this question can be answered positively, and the proposed device is surprisingly simple. It is a non-integer step phase plate carrying a straight edge dislocation, as shown in Fig. 5. Obviously, such a plate can be manufactured more easily than the spiral phase plates, whose production and characterisation is extensively discussed elsewhere [30, 31].
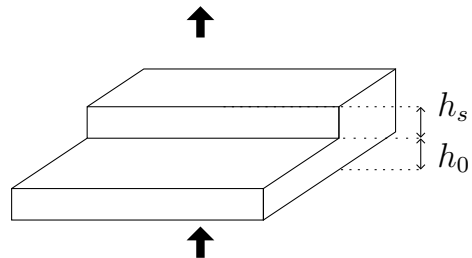

FIG. 5: Similar to the spiral phase plate in Fig. 1a), the non-integer step phase plate has its step height h_s chosen so that the phase shift due to the thick part is a non-integer multiple of 2π with respect to the thin part. The edge dislocation is chosen so that it goes through the centre of the field mode.

Similar to the non-integer spiral phase plate, the non-integer step phase plate contains an orientational degree of freedom, α. It is possible to write a unitary operator for the plate's action,

$$\langle x,y|\hat{\mathcal{F}}(\alpha,\phi)|l\rangle = \frac{\exp(il\theta)}{\sqrt{2\pi}} \times \begin{cases} \exp(i\phi), & \alpha \le \theta < \alpha + \pi, \\ 1, & \end{cases}$$

$$(19)$$

where $\alpha \in [0,\pi)$ represents the orientation of the step, ϕ the optical phase delay resulting from the step, $\theta \in [0,2\pi)$ the azimuthal angle and $|l\rangle$ the orbital angular momentum eigenstates. For the special case $\phi = \pi$, Eq. (19) corresponds to the Hilbert transform [32, 33]. The
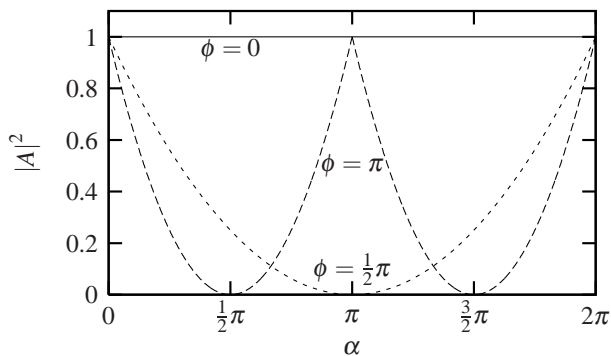
FIG. 6: The overlap (see Eq. (21)) between a state with an imprinted line dislocation, and the identical state rotated over α. When there is no dislocation ($\phi = 0$), the states are identical. For other phase differences ϕ, the two states are generally different; $\phi = \frac{1}{2}\pi$ and $\phi = \pi$ result in a continuous parabolic fringe.

non-integer step phase plate obviously also transforms the pure orbital angular momentum states into high-dimensional states, due to the edge dislocation. The definition as given here can be extended for $\alpha \in [-\pi, \pi)$, seemingly complicating matters, but without any impact on the calculations ahead.

Since the operator $\hat{\mathcal{F}}$ is unitary, we can define a new, complete basis $\left\{|b_\phi^{(l)}(\alpha)\rangle\right\}$, where $\hat{\mathcal{F}}(\alpha, \phi)|l\rangle = |b_\phi^{(l)}(\alpha)\rangle$. We can write the states after rotation $|b_\phi^{(l)}(\alpha)\rangle$ in terms of superpositions of the non-rotated states, $|b_\phi^{(l)}(0)\rangle$, where the decomposition depends on the angle α. We can illustrate this by making a projection of such a state with $\alpha = 0$ onto the same state $\alpha \neq 0$. The overlap amplitude thus becomes

$$
\begin{aligned}
A(\alpha) &= \langle b_\phi^{(l)}(0)|b_\phi^{(l)}(\alpha)\rangle \\
&= \frac{\alpha}{\pi}(\cos\phi - 1) + 1,
\end{aligned}
\tag{20}
$$

which is valid for values of $\alpha \in [-\pi, \pi)$. The overlap probability is given by

$$
|A(\alpha)|^2 = \left(\frac{\alpha}{\pi}\right)^2(\cos\phi - 1)^2 + 2\frac{\alpha}{\pi}(\cos\phi - 1) + 1. \tag{21}
$$

Figure 6 shows the intensity fringe as a function of α for three different values of ϕ. For clarity, we show the functions over the range $\alpha \in [0, 2\pi)$ instead of $\alpha \in$

$[-\pi, \pi)$, which is allowed when α is periodic over 2π. The most interesting cases occur when $\phi = \pi$ and $\phi = \pi/2$, when the fringe becomes a parabola, periodic over π and 2π, respectively. The result is then, aside from the periodicity, identical to that for a half-integer spiral phase plate.

A plate with a single edge dislocation with phase difference π or $\pi/2$ can thus be used, similar to a spiral phase plate, to investigate entanglement. The setup would be identical to Fig. 2 with the spiral phase plates replaced by the edge dislocation devices discussed here. The calculation from two-photon state to coincidence fringe is the same as discussed in section VI, using the states $|b_\pi^{(l)}(\alpha)\rangle$, or $|b_{\pi/2}^{(l)}(\alpha)\rangle$ instead of $|a_{1/2}^{(l)}(\alpha)\rangle$.

The CHSH-Bell inequality is violated maximally for these two-photon states, using the set of sixteen angles as used in polarisation entanglement for $\phi = \pi$, and the set as used for the half-integer spiral phase plates for $\phi = \pi/2$. Both cases yield an CHSH-Bell parameter equal to $S = 3\frac{1}{5}$.

Finally, we note that binary phase plates only slightly more complex than the type discussed above and pictured in Fig. 5, can yield an even stronger violation of the CHSH-Bell inequality. When using a plate with the shape as indicated in the inset of Fig. 7, the maximum CHSH-Bell parameter will be equal to $S = 4$, the highest value at all possible. For such a plate, we predict a coincidence fringe with a shape as indicated in Fig. 7.
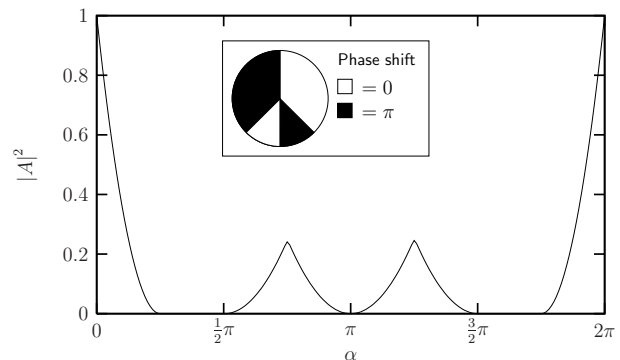

FIG. 7: When using a plate as indicated in the inset, the overlap (see Eq. (21)) as a function of α is as shown in the graph. This results in $S = 4$.

[1] L. Allen, M. W. Beijersbergen, R. J. C. Spreeuw, and J. P. Woerdman, Phys. Rev. A **45**, 8185 (1992).
[2] A. Mair, A. Vaziri, G. Weihs, and A. Zeilinger, Nature **412**, 313 (2001).
[3] A. Vaziri, G. Weihs, and A. Zeilinger, Phys. Rev. Lett. **89**, 240401 (2002).
[4] J. Preskill, Phys. Today **52**, 24 (1999).
[5] G. F. Brand, Amer. J. Phys. **67**, 55 (1999).
[6] I. Basistiy, V. Y. Bazhenov, M. S. Soskin, and M. V. Vasnetsov, Opt. Commun. **103**, 422 (1993).
[7] M. W. Beijersbergen, R. P. C. Coerwinkel, M. Kristensen, and J. P. Woerdman, Opt. Commun. **112**, 321 (1994).
[8] P. G. Kwiat, K. Mattle, H. Weinfurter, and A. Zeilinger,

Phys. Rev. Lett. **75**, 4337 (1995).

[9] S. J. van Enk and G. Nienhuis, Opt. Commun. **94**, 147 (1992).

[10] M. Abramowitz and I. A. Stegun, eds., *Handbook of mathematical functions* (Dover, New York, 1965).

[11] N. R. Heckenberg, R. McDuff, C. Smith, H. Rubinsztein-Dunlop, and M. J. Wegener, Opt. Quant. Elec. **24**, 5951 (1992).

[12] There do exist holograms that can generate mixed screw-edge dislocations in optical fields, thus modifying the OAM expectation value by non-integer numbers. See for these holograms, M. V. Vasnetsov, I. V. Basistiy and M. S. Soskin, in *International conference on singular optics*, (ed. M. S. Soskin) (SPIE-International Society for Optical Engineering, Bellingham, WA, 1998), vol. 3487 of SPIE Proceedings, pp. 29–33.

[13] H. H. Arnaut and G. A. Barbosa, Phys. Rev. Lett. **85**, 286 (2000).

[14] E. R. Eliel, S. M. Dutra, G. Nienhuis, and J. P. Woerdman, Phys. Rev. Lett. **86**, 5208 (2001).

[15] H. H. Arnaut and G. A. Barbosa, Phys. Rev. Lett. **86**, 5209 (2001).

[16] S. Franke-Arnold, S. M. Barnett, M. J. Padgett, and L. Allen, Phys. Rev. A **65**, 033823 (2002).

[17] G. A. Barbosa and H. H. Arnaut, Phys. Rev. A **65**, 053801 (2002).

[18] J. P. Torres, Y. Deyanova, L. Torner, and G. Molina-Terriza, Phys. Rev. A **67**, 052313 (2003).

[19] J. Visser and G. Nienhuis, Eur. Phys. J. D **29**, 301 (2004).

[20] J. Bell, Physics **1**, 195 (1964).

[21] N. D. Mermin, Phys. Rev. D **22**, 356 (1980).

[22] A. Peres, Phys. Rev. A **46**, 4413 (1992).

[23] D. Kaszlikowski, P. Gnaciński, M. Żukowski, W. Miklaszewski, and A. Zeilinger, Phys. Rev. Lett. **85**, 4418 (2000).

[24] T. Durt, D. Kaszlikowski, and M. Żukowski, Phys. Rev. A **64**, 024101 (2001).

[25] D. Collins, N. Gisin, N. Linden, S. Massar, and S. Popescu, Phys. Rev. Lett. **88**, 040404 (2002).

[26] J. F. Clauser, M. A. Horne, A. Shimony, and R. A. Holt, Phys. Rev. Lett. **23**, 880 (1969).

[27] A. Peres, *Quantum theory: concepts and methods* (Kluwer Academic Publishers, Dordrecht, 1993).

[28] A. Garuccio and V. A. Rapisarda, Nuovo Cimento **65A**, 269 (1981).

[29] J. F. Clauser and M. A. Horne, Phys. Rev. D **10**, 526 (1974).

[30] S. S. R. Oemrawsingh, J. A. W. van Houwelingen, E. R. Eliel, J. P. Woerdman, E. J. K. Verstegen, J. G. Kloosterboer, and G. W. 't Hooft, Appl. Opt. **43**, 688 (2004).

[31] S. S. R. Oemrawsingh, E. R. Eliel, J. P. Woerdman, E. J. K. Verstegen, J. G. Kloosterboer, and G. W. 't Hooft, J. Opt. A **6**, S288 (2004).

[32] A. N. Oppenheim and R. W. Shafer, *Digital Signal Processing* (Prentice-Hall, Englewood Cliffs, New Jersey, 1975).

[33] S. N. Khonina, V. V. Kotlyar, M. V. Shinkaryev, V. A. Soifer, and G. V. Uspleniev, J. Mod. Opt. **39**, 1147 (1992).